INFECTION AND IMMUNITY, June 1998, p. 2928–2937 Vol. 66, No. 6
0019-9567/98/$04.00+0


# Physical Limitations on *Salmonella typhi* Entry into Cultured Human Intestinal Epithelial Cells

XIAO-ZHE HUANG,[1] BEN TALL,[2] WILLIAM R. SCHWAN,[1]† AND DENNIS J. KOPECKO[1]*

*Laboratory of Enteric and Sexually Transmitted Diseases, Center for Biologics Evaluation and Research, Food and Drug Administration, Bethesda, Maryland 20892,[1] and Division of Microbiological Studies, CFSAN, Food and Drug Administration, Washington, DC 20204[2]*

Received 27 August 1997/Returned for modification 6 November 1997/Accepted 5 March 1998

**Kinetic studies of *Salmonella typhi* invasion of INT407 cells at different multiplicities of infection (MOIs) have revealed a strict physical limitation on *S. typhi* entry at MOIs of ≥40. Staining of infected monolayers to distinguish intracellular from extracellular bacteria revealed that all monolayer cells are susceptible to infection and that internalized bacteria are typically contained in one to three separate clusters per cell during the first 60 min. Scanning and transmission electron microscopic analyses of time course-infected monolayers showed that at early times postinfection, bacteria bind to shortened, coalesced microvilli in one to three focal aggregate structures per host cell surface. As reported previously for *S. typhimurium*, focal aggregates progress to conical membrane ruffles that appear to engulf one or a few centrally contained *S. typhi* cells by a macropinocytic process, which enhanced the entry of simultaneously added *Escherichia coli* HB101 about 30-fold. Additionally, kinetic studies showed that at an MOI of ≃400, maximal *S. typhi* entry is virtually completed within 30 to 35 min. Monolayers pretreated with *S. typhi* for 30 min to saturate the entry process were severely reduced in the ability to internalize subsequently added kanamycin-resistant strains of *S. typhi* or *S. typhimurium*, but *E. coli* HB101(pRI203) expressing the cloned *Yersinia inv* gene was not reduced in entry. In invasion inhibition assays, anti-β1 integrin antibodies markedly reduced *E. coli* HB101(pRI203) invasion efficiency but did not reduce *S. typhi* entry. Collectively, these data provide direct physical and visual evidence which indicates that *S. typhi* organisms are internalized at a limited number (i.e., two to four) of sites on host cells. *S. typhi* and *S. typhimurium* likely share INT407 cell entry receptors which do not appear to be members of the β1 integrin superfamily.**

Bacterial invasion of the host intracellular environment is an essential early step in the pathogenesis of invasive bacterial enteric diseases such as bacillary dysentery and typhoid fever (34, 38). Studies conducted over the past 15 years have shown that microbe-directed entry into mammalian intestinal epithelial cells is the result of specific interactions of bacterial determinants (e.g., adherence factors and invasion ligands) with host cell surface receptors (5, 10, 11, 17, 18, 21, 24). Apparently, effective invasion ligand-receptor interaction triggers a host cell signal transduction cascade that results in host cell membrane and cytoskeletal rearrangements leading to internalization of the adjacent pathogenic bacteria (5, 6, 10).

*Salmonella typhi*, the human-specific, causative agent of typhoid fever, continues to be a major global health problem. The World Health Organization has recently estimated that there are more than 16.6 million typhoid cases per year worldwide, equaling an annual incidence of >0.5% of the population and causing nearly 600,000 deaths yearly (35). *S. typhi*, an enterically acquired invasive pathogen, is thought to penetrate the ileal epithelium and be transported via underlying macrophages to the spleen, liver, and other target tissues during the normal disease course. Although antibiotic therapy can be used successfully to treat typhoid patients, natural clearance of the disease is thought to entail development of specific humoral and cellular immune responses. The precise mechanisms of *S. typhi* virulence and immune protection are not well understood, mainly due to the absence of a suitable animal model. Although limited studies of *S. typhi* virulence have been conducted (4, 42, 43), more emphasis has recently been placed on studying *S. typhimurium* virulence for mice, a surrogate model of typhoid. This later approach has revealed a large number of virulence genes in *S. typhimurium* (2, 11, 13, 22, 36), which were subsequently shown to exist in *S. typhi* (12). Despite harboring many similar virulence functions, these two *Salmonella* serovars trigger distinctly different disease syndromes in humans, a reminder of the limitations of any one experimental approach. We have been using cultured human epithelial cell lines to study the invasion mechanisms of *S. typhi* (4, 33). Biochemical inhibitor studies have revealed that *S. typhi* internalization is a microfilament-dependent process that is not affected by compounds which block endosome acidification or coated-pit formation but which requires bacterial nascent protein synthesis (33). The current picture of *S. typhi* invasion of human epithelial cells is sketchy and based on only a few specific studies of *S. typhi* (4, 20, 30, 42, 43) and on comparative analyses of *S. typhimurium* versus *S. typhi* invasion of cultured cells (12, 28).

This study was undertaken to analyze kinetically and microscopically the *S. typhi* invasion process, to gain information about receptor and entry sites, and to obtain a better physical understanding of *S. typhi* internalization. These new studies extend previous observations on the kinetics of *Salmonella* sp. entry into cultured epithelial cells (21) and suggest that a very limited number of *S. typhi* receptors and entry sites exist per cell. Moreover, the *S. typhi* entry sites on INT407 cells are apparently shared with those of the related serovar *S. typhimurium* but not with the *Yersinia* invasin-mediated uptake pathway.

* Corresponding author. Mailing address: Laboratory of Enteric and STD's, HFM 440, FDA-CBER, Bldg. 29, NIH Campus, Bethesda, MD 20892. Phone: (301) 496-1893. Fax: (301) 402-2776. E-mail: KOPECKO@A1.CBER.FDA.GOV.

† Present address: Pathogenesis Corp., West Seattle, WA 98119.

## MATERIALS AND METHODS

**Bacteria, human cell lines, and culture conditions.** Wild-type, virulent *S. typhi* Ty2 and Ty2W (a spontaneous Vi capsule-negative isogenic derivative) were obtained originally from the Walter Reed Army Institute of Research strain collection. Both strains were used in the cell culture invasion assay described below, but the Ty2W strain consistently showed higher (~2-fold) invasion ability and was used in all studies reported herein. An isogenic, kanamycin-resistant ($Km^r$) *S. typhi* Ty2W containing Tn*5* inserted in the *srlC* gene (Ty2W-154), constructed by Eric Elsinghorst (University of Kansas), was used in certain invasion competition assays.

*Escherichia coli* HB101 strains, a noninvasive *E. coli* K12/B genetic hybrid strain and an ampicillin-resistant ($Amp^r$) derivative of HB101 (from E. Elsinghorst), were used as negative experimental controls in invasion assays. *E. coli* HB101(pRI 203), provided by R. Isberg (Tufts University), contains the functional *Yersinia* invasin gene cloned into a plasmid which specifies both $Amp^r$ and chloramphenicol resistance ($Cm^r$) and was selected on LB medium containing these antibiotics. The highly mouse-virulent *S. typhimurium* strain 446, a C5 derivative containing Tn*5* inserted into *srlC*, was provided by E. Elsinghorst.

Bacteria, typically maintained as frozen stock cultures at −80°C in L broth containing 10% dimethyl sulfoxide, were grown at 37°C in L broth (Gibco/BRL) containing NaCl (10 g/liter) or L broth containing kanamycin (50 μg/ml; Sigma), ampicillin (50 μg/ml; Sigma), or chloramphenicol (20 μg/ml; Sigma) in tubes aerated slightly at 180 rpm to mid-log phase (optical density at 600 nm of ≈0.4 to 0.6) for invasion assays.

Because *S. typhi* normally invades the ileal epithelial mucosa in vivo and very efficiently invades cultured human embryonic intestinal 407 epithelial cells, INT407 cells were chosen as the in vitro model system. Realizing the experimental advantages and limitations of cultured host cell systems, we paid considerable attention to consistency of assay conditions, the use of invasion-positive and -negative controls, tissue culture viability and integrity assays, and exhaustive experimental repetition. INT407 cells (American Type Culture Collection, Rockville, Md.) were cultured in minimal essential medium (Gibco) with heat-inactivated 10% fetal calf serum (Gibco) and 2 mM L-glutamine (Gibco) under 5% $CO_2$ (Heraeus incubator type BB15) in 75-$cm^2$ tissue culture flasks maintained at 37°C. Monolayers were trypsinized, washed, and split 1:4 into fresh culture medium. Diluted cells reached confluency within 3 days, at which point they were used in invasion assays; these are young, confluent monolayers exhibiting surface microvilli.

**Invasion assays.** The invasion assay was performed as described previously (4, 33) except that the invasion period was reduced and the bacterial inoculum was not centrifuged to initiate contact with epithelial cells. Serial dilutions or centrifuged concentrates of freshly grown, log-phase bacteria suspended in 1× phosphate-buffered saline (PBS; Gibco) were prepared for each assay to reach estimated ranges of multiplicities of infection (MOIs) from ~0.4 bacteria per epithelial cell (i.e., MOI of ~0.4) to an MOI of ~4,000. Bacteria in 25 μl of PBS were added to confluent INT407 cell monolayers in 24-well tissue culture plates (Sarstedt, Inc.); each well, as assessed by representative hemocytometer counts of sample wells, contained ~$6 \times 10^5$ INT407 cells in 1 ml of medium. For most studies, the infected monolayers were incubated in 5% $CO_2$ at 37°C for 1 h to allow bacterial invasion to occur, washed twice for 1 min with 1 ml of minimal essential medium and then incubated for an additional hour in 1 ml of tissue culture medium containing gentamicin (100 μg/ml) to kill the remaining extracellular bacteria. For indirect measurement of bacterial invasion ability, the infected monolayers were washed as described above and lysed with 1 ml of 0.1% Triton X-100 for 10 min. After serial dilution in PBS, released intracellular bacteria were quantitated by viable count after growth for 24 h on L agar or, when necessary, L agar containing appropriate antibiotics. Bacterial invasion ability, expressed as invasion efficiency, was calculated as (number of internalized bacteria at the end of the assay/starting inoculum) × 100. All assays were conducted in duplicate and repeated independently at least three times. Results are expressed as the mean ± standard error of the mean of the replicate experiments. In some cases, invasion levels were compared by the Student *t* test for statistically significant differences. Consistent monolayer integrity and viability were verified at the end of the invasion assay period by standard trypan blue staining and microscopic analysis. Limited monolayer detachment was observed at the highest MOI of 4,000, and corrections to account for detached cells were made to estimate the total number of internalized bacteria.

**AO-CV staining.** The assay was conducted basically as described previously (25–27) to visualize live versus dead, intracellular as well as extracellular bacteria. INT407 monolayers were grown on 1.2-cm-diameter, sterile glass coverslips (Fisher Scientific) placed in well bottoms of 24-well tissue culture plates and incubated under the conditions described above. Briefly, the coverslips containing monolayers were infected with *S. typhi* for different times. These time course-infected monolayers on coverslips were stained with 0.01% acridine orange (AO) in Gey's solution (prepared according to the Gibco/BRL formula for slides) for 45 s, rinsed in 1× Dulbecco's PBS (DPBS; Gibco/BRL), and counterstained with 0.5% crystal violet (CV) in 0.15% NaCl for 45 s before washing with 1× DPBS. These preparations were wetted with tissue culture medium, mounted (with the monolayer side facing down) on glass microscope slides, and sealed with nail polish before viewing under a Zeiss Axioplan fluorescence microscope using halogen illumination and an Omega triple-band filter no. 0-5855 (Molecular Probes, Inc.). Under these conditions, viable intracellular bacteria stain bright green, nonviable intracellular bacteria stain red/orange, and extracellular bacteria counterstain deep violet/black. All bacteria internalized within a host cell could not typically be observed at any one focal plane. Thus, multiplanar focusing was used to view and enumerate all bacteria within the three-dimensional monolayer. Fluorescent bacteria in at least 30 separate cells in several different fields of view were assessed at each time point to determine the average number of intracellular bacteria per epithelial cell and the distribution of bacteria within the host cell. Internalized fluorescent bacteria were photographed with a microscope-mounted Zeiss MC100 camera using Kodak EPH p1600 film and an autoadjusted exposure control system.

**Competitive inhibition of invasion.** INT407 monolayers were first infected with *S. typhi* Ty2W at an MOI of 400, and then either competing $Km^r$ *S. typhi* Ty2W-154, *E. coli* HB101(pRI203), or *S. typhimurium* C5 *srlC*::Tn*5* bacteria were added at the same MOI either at the same time as Ty2W was added or 20 and 30 min after the addition of Ty2W. Invasion of the competing strain was allowed for 30 additional min, followed by a 60-min gentamicin kill period before enumeration of internalized competing bacteria on appropriate antibiotic-containing LB agar. Control invasion assays with $Km^r$ Ty2W-154, HB101(pRI203), or the $Km^r$ *S. typhimurium* C5 *srlC*::Tn*5* strain were carried out on previously uninfected INT407 cells. Monolayer integrity and viability were verified as noted above.

**Anti-integrin inhibition assay.** The procedure was similar to the standard invasion assay (17) except that 96-well plates were used. One of several anti-integrin monoclonal antibodies (MAbs) was added to 200 μl of medium covering a monolayer of approximately $7 \times 10^4$ INT407 cells in a well of a 96-well plate 60 min prior to initiation of the invasion assay. Then ~$1.5 \times 10^6$ bacteria (MOI of ≈20) were added to each treated monolayer. After a 1-h invasion period and a 1-h gentamicin treatment period, the intracellular bacteria were enumerated by viable count as described above. The anti-integrin α3β1, α4β1, and α5β1 MAbs (DAKO Corp., Carpinteria, Calif.) were dialyzed twice against 1,000 ml of PBS (pH 7.4) overnight at 4°C to remove the azide preservative and were maintained at 4°C. Anti-integrin β1 and α5 MAbs (kindly supplied by Kenneth Yamada, National Institute for Dental Research, Bethesda, Md.) were also tested.

**Electron microscopy (EM).** For scanning EM (SEM), INT407 monolayers were grown on 1.2-cm-diameter glass coverslips in 24-well tissue culture plates. After various incubation periods with *S. typhi* Ty2W (MOI of 40 or 400), the infected monolayers (without a gentamicin kill period) were washed twice with DPBS and then fixed by adding 1 ml of 3% glutaraldehyde in 0.1 M sodium cacodylate buffer (pH 7.2) and incubating the mixture for 24 h at 4°C. The coverslips were removed and processed for SEM by standard procedures and examined in an ISI Super IIIA scanning EM operating at an acceleration voltage of 15 kV (27, 39).

For transmission EM (TEM), monolayers were grown in six-well plates under the conditions described above for the invasion assays. The time course-infected monolayers were washed, fixed in 1 ml of 3% glutaraldehyde in sodium cacodylate buffer for 1 h at 4°C, harvested from the wells with a rubber scraper, and centrifuged in a microcentrifuge tube at 14,000 × *g* for 5 min at room temperature, and the pellet was resuspended in fixative and processed for TEM (39). The samples were evaluated with a Philips 400 HM TEM operating at an acceleration voltage of 80 kV as described by Oelschlaeger and Tall (31).

## RESULTS

**Effect of MOI on invasion efficiency versus number of bacteria internalized.** To monitor the effect of available bacteria on uptake, the invasion efficiency of *S. typhi* Ty2W was assessed over a wide range of starting MOIs, from approximately ≈0.4 to ≈4,000 bacteria per INT407 cell, by using the gentamicin kill-indirect plate count method. The resulting invasion efficiency increased steadily from a starting MOI of ≈0.4 to ≈40, where it reached a maximum of 48.9% and decreased sharply and consistently thereafter (Fig. 1A). The invasion efficiency was markedly lower at MOIs of ≈400 and ≈4,000 than at MOIs of 4 and 40. In contrast, the noninvasive control strain *E. coli* HB101 showed less than 0.001% invasion efficiency at all of the same MOIs (data not shown).

A strikingly different curve (Fig. 1B) resulted upon monitoring the total number of bacteria internalized relative to various MOIs in a log-versus-log plot. The total number of intracellular bacteria recovered from each well of infected monolayer host cells increased notably from an MOI of ≈0.4 to ≈40 but reached statistical saturation at an MOI of ≥40. The low level of *E. coli* HB101 entry in concurrent assays was unchanged over the various MOIs (data not shown). Thus, the invasion efficiency decreased sharply above an MOI of 40, but

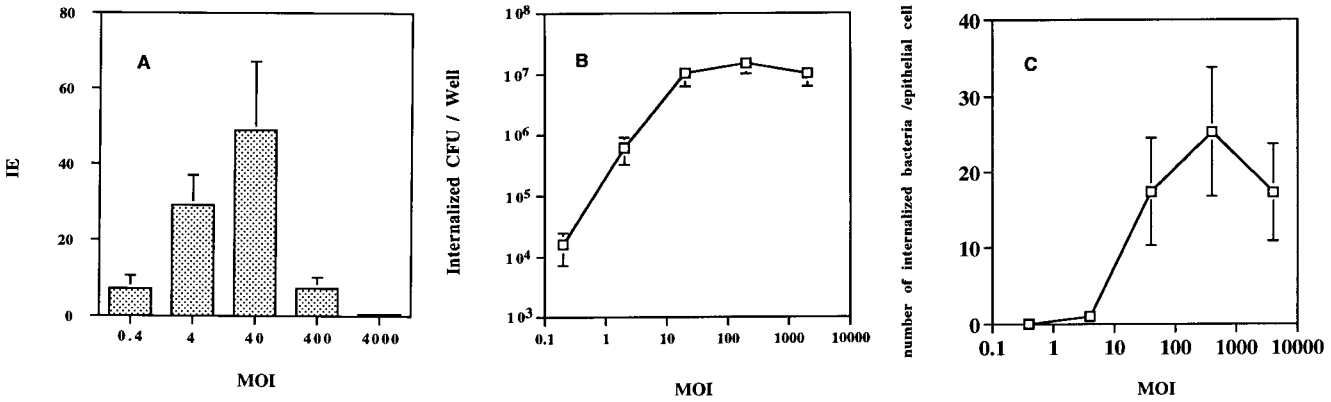


FIG. 1. Comparative study showing the effect of the *S. typhi* starting MOI on invasion efficiency (IE) versus the number of bacteria internalized into INT407 cells. (A) Effect of varying the starting MOI on *S. typhi* Ty2W invasion efficiency. Invasion assays were conducted, as described in Materials and Methods, testing a range of starting bacterial concentrations (expressed as the MOI of added bacteria per epithelial cell) and utilizing a 1-h invasion period and a 1-h gentamicin kill period prior to plate count enumeration of internalized bacteria. Invasion efficiency was calculated as percentage of the inoculum internalized at the end of the assay. All assays were conducted in duplicate and repeated on separate days at least three times. Results are presented as the mean invasion efficiency ± standard deviation. The invasion efficiency at an MOI of ~400 or ~4,000 was statistically lower than that at an MOI of ~40 ($P < 0.01$) or at an MOI of ~4 ($P < 0.01$). (B) Effect of varying the starting MOI on total *S. typhi* Ty2W internalized. Invasion assays were conducted as described above. Total number of internalized *S. typhi* bacteria resulting per assay well is expressed as CFU/well. All assays were conducted in duplicate and repeated on separate days at least three times. Results are presented as the mean number of CFU/well ± the standard deviation. The number of CFU/well obtained at MOIs of ~40 to ~4,000 was significantly increased over the number of CFU internalized at lower starting MOIs ($P < 0.01$). (C) Effect of varying the MOI on the resulting number of internalized bacteria averaged per epithelial cell. Invasion assays were conducted as described above. The total number of *S. typhi* Ty2W bacteria internalized per assay well is expressed as an average number of bacteria internalized per epithelial cell (i.e., by dividing the total number of internalized bacteria by the $6 \times 10^5$ epithelial cells in each well). All assays were conducted in duplicate and repeated on separate days at least three times. Results are presented as the mean of the average number of bacteria/epithelial cell ± the standard deviation. The resulting averaged number of bacteria/epithelial cell at MOIs of ~40 to ~4,000 was significantly ($P < 0.01$) increased over the results obtained at lower starting MOIs.

the total number of CFU of internalized *S. typhi* remained relatively constant above this inoculum size, suggesting a stringent limitation on entry at MOIs of ≥40.

Interestingly, when the number of internalized bacteria resulting from varying the starting MOI is expressed as the number of internalized CFU averaged per epithelial cell (Fig. 1C), a starting MOI of 40 resulted in a weighted average of ≃17 internalized bacteria per epithelial cell. This number increased slightly to peak at an average of ≃25 bacteria per epithelial cell at an MOI of ≃400.

**Direct quantitation of *S. typhi* internalization by fluorescence microscopy.** The gentamicin kill procedure has been used in conjunction with invasion assays to kill extracellular bacteria after the invasion period and before indirect bacteriologic viable count determination. Although the method is accepted by many, there is some question of whether the bacteriologic plate count represents an accurate reflection of internalized bacteria. The following analyses were initiated to obtain a direct visual assessment of internalized bacteria and to examine the number of host cells infected over time.

Representative INT407 monolayers were infected with *S. typhi* Ty2W and monitored for internalized bacteria at various times postinfection (Table 1) by using the following methods. One set of infected monolayers was treated with gentamicin for 1 h (gentamicin kill period) before viable count enumeration of internalized bacteria. Another set of time course-infected monolayers was examined directly by AO-CV staining and fluorescence microscopic analysis (Table 1). As assessed by the indirect plate count method, 1.2% of the inoculum at an MOI of ≃40 was internalized during the first 10 min, and this

TABLE 1. Time course comparative enumeration of *S. typhi* internalized into INT407 cells[a]

| Time (min) | Plate count assay | | AO-CV assay | | |
|---|---|---|---|---|---|
| | IE (%) (mean ± SEM) | No. of bacteria/cell (mean ± SEM) | % INT407 cells infected | Avg (predicted) no. of bacteria/cell (mean ± SEM) | No. of foci/cell (mean ± SEM) |
| 0 | 0 | 0 | 0 | 0 | 0 |
| 10 | 1.2 ± 0.3 | 0.3 ± 0.1 | 10 | 1.9 ± 0.8 (0.4) | ND |
| 20 | 6.5 ± 2.5 | 1.9 ± 0.9 | ND | ND | ND |
| 30 | 13.7 ± 3.2 | 3.5 ± 0.9 | 81 | 4.1 ± 2.1 (6.6) | 2.1 ± 0.8 |
| 45 | 21.1 ± 6.2 | 5.9 ± 1.3 | ND | ND | ND |
| 60 | 54.9 ± 15.2 | 14.9 ± 2.0 | 100 | 7.7 ± 2.4 (15.4) | 2.3 ± 0.8 |

[a] INT407 monolayers were infected with *S. typhi* Ty2W at an MOI of ~40 for various times and then analyzed for internalized bacteria by one of two methods. For indirect plate count determination, the infected monolayers were washed, incubated for a further 1 h in fresh medium containing gentamicin (100 μg/ml), and then lysed with Triton X-100 before viable count assay as described in Materials and Methods. Bacterial entry is expressed as invasion efficiency (IE) and the number of internalized bacteria averaged per INT407 cell. Alternatively, a second set of monolayers infected for various times were washed, stained, and directly observed by fluorescence microscopy. These stained monolayers were assessed for percentage of monolayer cells infected over time, the number of internalized bacteria averaged per infected cell, and the number of clusters (i.e., infection foci) of internalized bacteria. The numbers in parentheses represent the predicted average numbers of bacteria per cell which would be comparable to the data obtained by plate count assay. These determination were made by taking the actual number obtained by AO-CV assays, averaging the bacteria internalized over the entire monolayer (i.e., 2 bacteria per infected cell at 10 min, where 10% of the monolayer is infected would be equivalent to 0.2 bacteria/cell averaged over the entire monolayer), and multiplying by 2 to allow for estimated bacterial multiplication that occurred during the extra 1-h gentamicin kill period in the plate count assay. ND, not determined.

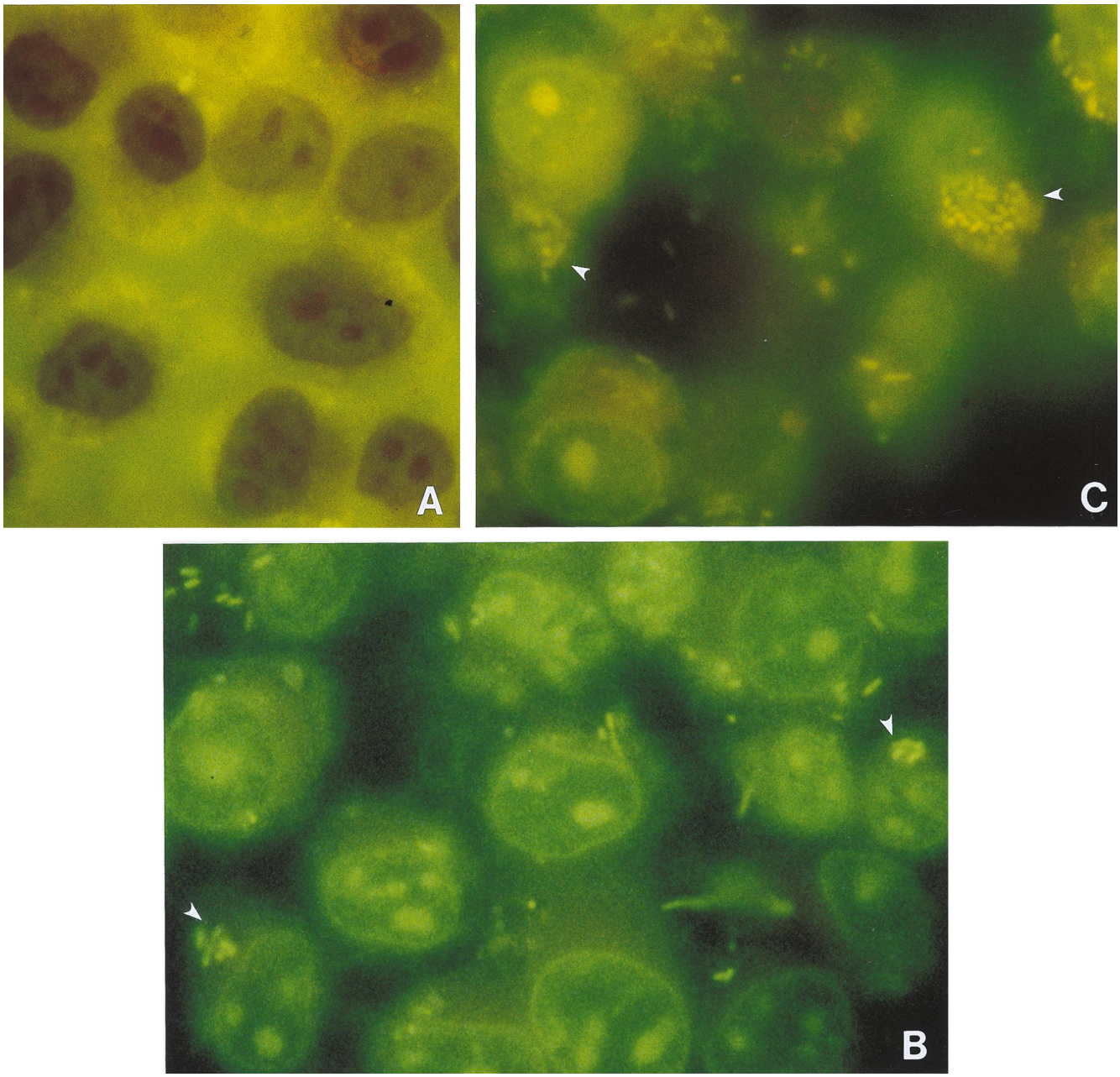


FIG. 2. AO-CV staining of *S. typhi*-infected INT407 monolayers. Representative fluorescence micrographs of AO-CV-stained INT407 monolayers infected with *S. typhi* Ty2W at an MOI of ~400 at time zero (A), 20 min postinfection (B), or 45 min postinfection (C). Observe the green, live intracellular *S. typhi* within epithelial cells. Dark violet-counterstained, extracellular bacteria were observed at the highest focal planes but are not seen at the focal planes photographed here. The arrowheads in panels B and C point to clusters of internalized bacteria, each of which is referred to as an infection focus. As described in Materials and Methods, all bacteria within a cell could only be assessed by multiplanar focusing, but the photos necessarily represent only one focal plane.

invasion efficiency increased steadily to a level of ~55% at 60 min (Table 1). Using the total number of bacteria internalized per assay well divided by $6 \times 10^5$ monolayer cells per well, we calculated the number of internalized bacteria averaged per epithelial cell; however, 100% of the monolayer cells were infected only after 60 min.

Figure 2 shows representative photomicrographs of AO-CV-stained monolayers after various times postinfection with *S. typhi* at an MOI of ≃400. We observed a gradual increase in the number of green fluorescent, live, intracellular bacteria over time. Dark violet-counterstained, extracellular bacteria were occasionally observed at higher focal planes on top of the INT407 cells (data not shown). For each experiment, 100 monolayer cells were scanned to determine the percentage of infected versus noninfected INT407 cells. At an MOI of ≃40, the percentage of infected INT407 cells increased from 10 at 10 min postinfection to 100 at 60 min (Table 1). Also presented are the means of the number of intracellular bacteria visualized per infected INT407 cell, which were 1.9 at 10 min postinfection and 7.7 after 60 min. The numbers of bacteria visualized internally within INT407 cells over time correlated well with expectations based on the indirect bacterial counts shown

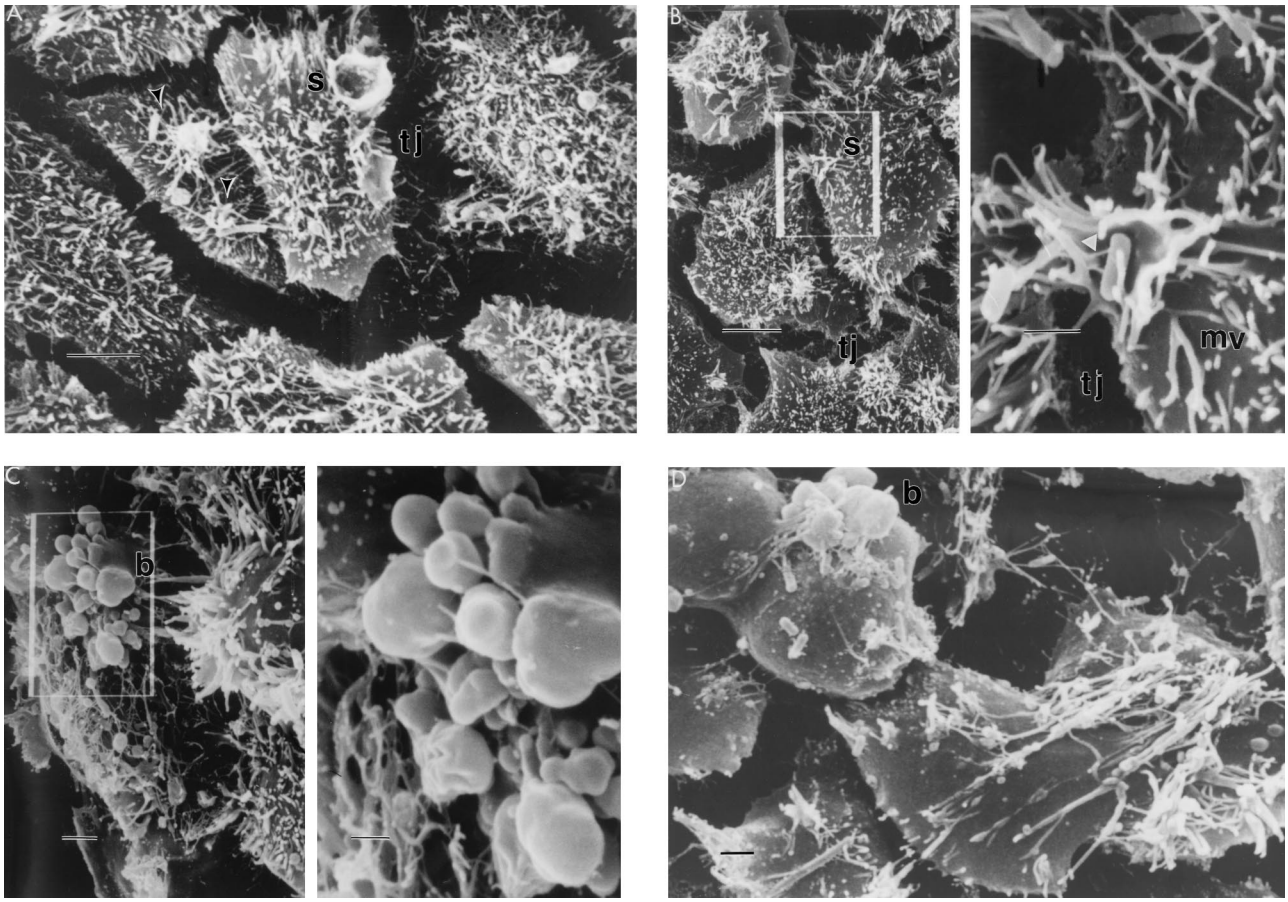


FIG. 3. Representative scanning electron photomicrographs of *S. typhi* internalization into INT407 cells at various times postinfection at an MOI of ≃400. Panels B and C are composite photos with the lower-magnification image on the left containing a boxed area that is amplified on the right. Microvilli (mv), membrane splash (s), tight junction (tj), and membrane bleb (b) are indicated. (A) Monolayer at 10 min postinfection, showing focal aggregates of bound bacteria (arrowheads) and membrane splashes. The normal tight junction appears as a junctional space, created by host cell contraction during sample preparation. (B) At 20 min postinfection, two to three focal aggregates per cell can be observed adjacent to the tight junction. Amplification of a focal aggregate shows the beginnings of a membrane splash with bacteria attached to the host cell membrane via coalesced microvilli and thinner structures (arrowhead) of undefined origin. (C) At 45 min postinfection, the INT407 cell surface is denuded and many surface membrane alterations or blebs as well as some surface bound bacteria can be seen. (D) By 60 min postinfection, most epithelial cells appeared swollen and heavily denuded of microvilli, but with some bound bacteria. Bar markers: A to C (low-magnification photos), 5 μm; B and C (high-magnification photos), 1 μm; D, 2 μm.

in Table 1. In the indirect plate count invasion method, the internalized bacteria had an extra hour to multiply during the gentamicin kill period and would have doubled during this time, according to control studies (data not shown). Thus, 7.7 bacteria per INT407 cell at 60 min enumerated by the direct AO-CV method (which did not contain a gentamicin kill period) was, as expected, about half of the 14.9 bacteria per cell obtained by indirect plate count. Additionally, limited invasion studies were conducted in duplicate, and infected monolayers were treated with a gentamicin kill period prior to enumeration by indirect plate count versus direct visualization methods, resulting in virtually identical results (data not shown). Thus, both methods of calculating internalized bacteria gave equivalent results at an MOI of ≃40. Similar time course studies carried out at an MOI of ≃400 showed that bacterial entry increased more quickly with time and that 100% of the monolayer was infected within ~30 min at this MOI (data not shown).

In addition, the AO-CV method revealed an unexpected observation in which the internalized bacteria existed in a limited number of clusters or foci of infection as exemplified in Fig. 2 (MOI of ≃400) and summarized in Table 1 (MOI of ≃40). There were an average of 2 ± 1 foci of infection (i.e., cluster of bacteria) per infected INT407 cell at 30 and 60 min postinfection at an MOI of ≃40. The only difference between early and late time points was a larger number of bacteria per infection focus at later times postinfection, probably due to intracellular bacterial replication (Table 1). After infection at an MOI of ≃400, infection foci per cell still averaged between 2.0 and 2.5 at both early and later time points (data not shown). These data suggest that *S. typhi* entry is kinetically saturable and may occur at a limited number of possible entry points per INT407 cell, each of which results in an infection focus.

**Analysis of *S. typhi* internalization by SEM and TEM.** To obtain more detailed information about the events and structures associated with *S. typhi* entry, time course-infected monolayers infected with *S. typhi* at an MOI of ≃40 or ≃400 were examined by both SEM and TEM (Fig. 3 and 4). At time zero, SEM revealed typical, young confluent monolayer cells containing many apical microvilli (data not shown). By 10 min postinfection, bacterial cells could be seen attached to the INT407 cell surface as focal aggregates of one or, typically, two bacteria bound to shortened and coalesced microvilli (Fig. 3A). These focal aggregates, commonly observed adjacent to the

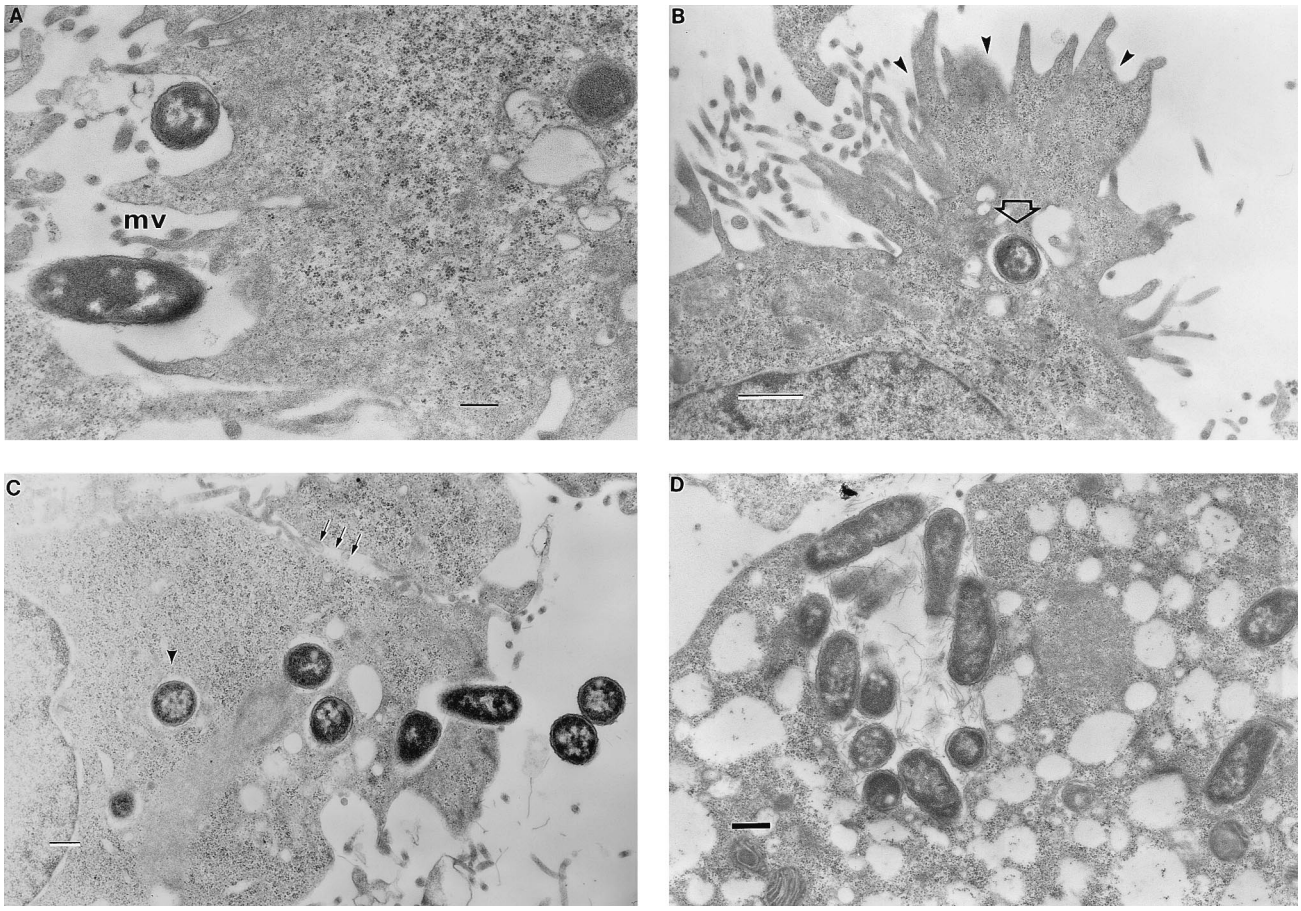


FIG. 4. Representative transmission electron photomicrographs of INT407 monolayers infected over time with *S. typhi* at an MOI of 400. (A) At 10 min postinfection, bacteria are observed interacting with shortened microvilli (mv) in apparent early focal aggregate structure. (B) 20 min postinfection. Cross-sectional view of a bacterium (open arrow) being engulfed in a host cell membrane splash (arrowheads). (C) 30 min postinfection. Multiple bacteria being internalized at one apical site which is adjacent to the junctional space (arrows). At least one bacterium seems clearly to exist in a separate endosome (arrowhead). (D) 2 h postinfection. The entire monolayer shows the presence of numerous vacuoles as well as clusters of internalized bacteria. Bar markers: A, C, and D, 0.5 μm; B, 1 μm.

tight junction and seen under these conditions as white patches on the host cell surface, correlated well with the number of infection foci observed by AO-CV staining. A higher magnification of some focal aggregates showed early stages of membrane ruffling (i.e., splash) with bacteria bound to microvilli and also tethered by thinner structures of the size of bacterial flagella (Fig. 3B). More INT407 cells contained bound bacteria at earlier time points at an MOI of ≃400 than at an MOI of ≃40, as expected. One striking feature of these monolayers was that infected INT407 cells typically had between one and three focal aggregates of bound bacteria per cell, regardless of the starting MOI. The next structures observed chronologically after the formation of focal aggregates of bound bacteria were conical or splash-like protrusions of the INT407 apical cell membrane, which appeared to engulf centrally contained bacteria (Fig. 3A and B) as observed previously for *S. typhimurium* (7). These membrane splash structures, which possessed a distinct rim and associated coalesced microvilli, were observed as early as 10 min in monolayers infected at an MOI of ≃400 (Fig. 3A) but took typically 20 min or more to appear in monolayers infected at an MOI of ≃40 (data not shown).

At later times, the infected INT407 cells showed the expanded presence of small and large membrane blebs or protrusions, as well as large apical areas denuded of microvilli (Fig. 3C and D). Monolayer cells exhibiting these major surface membrane alterations, observed within 60 min at an MOI of ≃40, were viable as assessed by trypan blue staining. Even though bacteria can be seen bound apically to these dramatically altered host cells, bacterial entry was essentially completed in 1 h at an MOI of 40.

TEM studies were conducted to obtain a cellular, cross-sectional view of events occurring during *S. typhi* invasion of INT407 cells. At early times (10 to 30 min), surface-interacting *S. typhi* cells appear bound in early focal aggregate structures (Fig. 4A), which after effective contacts trigger membrane engulfment of adjacent bacteria into an enclosed endosome (Fig. 4B). Internalized salmonellae were bound by an endosomal membrane and did not appear to exist free in the cytoplasm, at least not during the first 2 h postinfection. Even at 10 or 30 min postinfection at an MOI of ~400, some endosomes contained multiple bacteria which may have been engulfed during a single entry event or could have resulted from vacuole fusion (Fig. 4C). This micrograph (Fig. 4C) is representative of several in which bacteria were observed to exist in clusters of separate endosomes, all close to the membrane site of active entry. It suggests that one to two bacteria may be engulfed per event and that several consecutive uptake events may take place at the same activated membrane site. At later times postinfection, most INT407 cells contained bacteria in two to three separate clusters as observed by direct visualization techniques, suggest-

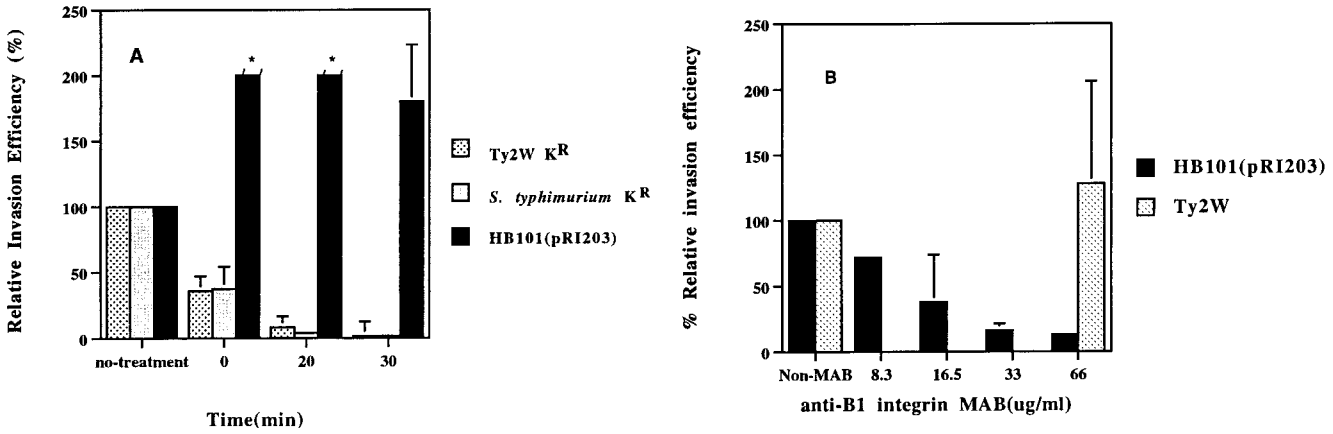


FIG. 5. Time course competitive inhibition of *S. typhi* invasion. (A) INT407 monolayers in 24-well tissue culture plates were first infected with *S. typhi* Ty2W at an MOI of ~400. Without washing the infected monolayer, a competing $Km^r$ Ty2W strain was added (also at an MOI ≃400) at time zero or after previous infection with Ty2W for 20 or 30 min. Competing strains *S. typhimurium* C5 *srlC*::Tn*5* and HB101(pRI203) were added separately at 0, 20, and 30 min, and the assay was conducted as described in Materials and Methods. Internalized bacteria are shown as total CFUs per assay well versus time of addition to the monolayer. This experiment was repeated three times and the data are expressed as mean CFU ± standard error of the mean. *, the response bar is off the scale of the graph. The relative invasion efficiencies of *E. coli* HB101(pRI203) were determined as 890% on average at 0 min and 380% on average after 20 min of pretreatment with *S. typhi* Ty2W. (B) Effect of anti-β1 integrin MAb on invasion of INT407 cells by *S. typhi* or *E. coli* expressing *Yersinia* invasin. Young confluent INT407 monolayers were prepared as described in Materials and Methods for standard 1-h invasion assays followed by a 1-h gentamicin kill period prior to plate count enumeration. However, untreated monolayers were compared to monolayers pretreated for 1 h with various concentrations of anti-β1 integrin mouse MAb for the ability to internalize either *S. typhi* Ty2W or *E. coli*(pRI203). In the absence of antibody pretreatment, *S. typhi* Ty2W invaded at ~50% invasion efficiency while the invasin-expressing *E. coli* invaded at ~2% invasion efficiency, both of which were considered 100% relative invasion efficiencies. Effect on invasion ability is expressed as percent relative invasion efficiency, which equals (invasion efficiency after pretreatment with antibody/invasion efficiency without pretreatment) ×100.

ing that the internalized bacteria do not coalesce into a single large endosome during the first 1 h but do so at later times as reported for other *Salmonella* serovars (8a). Finally, at 2 h postinfection at an MOI of ~40 or ~400, the infected monolayer cells contained clusters of bacteria and numerous empty vacuoles, possibly indicative of early stages of cell necrosis (Fig. 4D). Note that the cluster of internalized bacteria in Fig. 4D is associated with filamentous material as described previously for other *Salmonella* serovars (7).

**Does *S. typhi* trigger macropinocytosis?** To ascertain if the broad membrane ruffling or associated signal transduction events of INT407 cells induced by *S. typhi* and observed by both SEM and TEM somehow triggered the uptake of adjacent, noninvasive bacteria, the following study was conducted. A standard 1-h invasion assay was initiated by simultaneously adding *S. typhi* Ty2W (MOI of ≃40) and the noninvasive *E. coli* HB101 $Amp^r$ (MOI of ≃40), which was followed by a 1-h gentamicin kill period before viable count determination. The typical, very low invasion efficiency of *E. coli* HB101 (≤0.001% when HB101 is used alone) was enhanced ~30-fold during this coinfection study. In an additional study, INT407 monolayers were coinfected at equal MOIs of ≃40 with *S. typhi* Ty2W and *E. coli* HB101(pRI203). The HB101(pRI203) invasion level was enhanced ~4-fold over the normal invasion level of HB101(pRI203) alone (data not shown).

**Competitive inhibition studies of *S. typhi* invasion.** Time course analyses of *S. typhi* internalization into INT407 cells revealed that bacterial entry was essentially completed within 1 h at a starting MOI of ≃40 and within 30 to 35 min at an MOI of ≃400. We wondered if preinfected monolayer cells might be exhausted for further invasion by *S. typhi* or, perhaps, by other invasive bacteria. A time course, invasion competition study was conducted to examine the development of monolayer invasion exhaustion versus time. In this study, INT407 monolayers were first infected with *S. typhi* Ty2W at an MOI of ~400. Without any other manipulations, the competing $Km^r$ Ty2W-154 strain (at an MOI of ~400) was added to these monolayers either at time zero or after previous infection with Ty2W for 20 or 30 min. *E. coli* HB101(pRI203), which carries the cloned functional *Yersinia inv* locus, and $Km^r$ *S. typhimurium* C5 *srlC*::Tn*5* were also added to preinfected monolayers as described above at 0, 20, and 30 min after infection with Ty2W. Coinfection was allowed to continue for 30 min and was followed by a gentamicin kill period before enumeration of internalized $Cm^r$ or $Km^r$ bacteria. The number of $Km^r$ Ty2W bacteria internalized per well when added at time zero was about one-half of the typical invasion level of Ty2W-154 $Km^r$ by itself (Fig. 5A), demonstrating that Ty2W and Ty2W $Km^r$ compete equally well for entry when added together at similar MOIs. However, prior infection with the parental Ty2W increasingly reduced the invasion ability of the competing $Km^r$ Ty2W. Monolayers infected for 30 min with Ty2W and then infected with the isogenic $Km^r$ Ty2W showed a 2-log reduction in the $Km^r$ strain's ability to enter INT407 cells. A longer pretreatment time of 60 min reduced the competing Ty2W $Km^r$ strain entry by 3 logs (data not shown). The normal level of *S. typhimurium* C5 invasion was similarly and dramatically lowered by pretreatment of the INT407 monolayer with *S. typhi* (Fig. 5A). In contrast, preinfection with *S. typhi* did not cause any reduction in typical entry of *E. coli* (pRI203); entry of this recombinant strain was actually enhanced ~2- to 9-fold. Thus, preinfection of INT407 cells over time with *S. typhi* reduced the ability of these cells to further internalize *S. typhi* or *S. typhimurium* but did not limit *Yersinia* invasin-mediated entry.

To test whether pretreatment at a lower MOI would cause reduced invasion exhaustion and to examine saturation of invasion ability, monolayers were pretreated with Ty2W at an MOI of ≃10 for 1 h and washed before being (i) counterinfected with $Km^r$ Ty2W at an MOI of ≃10 for 1 h or (ii) grown in fresh medium containing gentamicin for 4 h and then counterinfected. This 1-h pretreatment condition reduced $Km^r$ Ty2W entry by 60%. Half of this inhibition was overcome by

the 4-h growth period prior to counterinfection (data not shown).

**Effect of anti-integrin antibodies on *S. typhi* invasion ability.** Previous studies (31) have shown that *S. typhi* invasion of epithelial cells, like uptake of *Yersinia*, *Shigella*, and *Listeria*, is dependent upon microfilaments. Structurally, microfilaments are connected with the eukaryotic cell surface via the membrane-spanning integrins (3). Furthermore, members of the β1 integrin superfamily have been shown to serve as receptors for the *Yersinia* invasin ligand (18). The following studies were performed to ascertain if any of several anti-integrin antibodies could block *S. typhi* invasion compared to *E. coli* HB101 (pRI203) internalization. Figure 5B summarizes the results of a representative assay. Without anti-integrin antibody, *S. typhi* and HB101(pRI203) were internalized with the expected invasion efficiencies of ~50 and ~2%, respectively. As expected, invasin-mediated uptake of HB101(pRI203) was inhibited by antibodies in a concentration-dependent fashion, showing >80% inhibition at anti-β1 integrin antibody concentrations of 33 and 66 μg/ml. However, *S. typhi* entry into INT407 cells was not inhibited, even when 66 μg of anti-β1 integrin antibody per ml was added. Similarly, mouse anti-α3β1, -α4β1, -α5β1, and -α5 MAbs were all found to inhibit *Yersinia* invasin-mediated entry but not *S. typhi* invasion (data not shown).

## DISCUSSION

Investigations over the past 15 years stimulated largely by advances in cellular and molecular biology have refocused on the pathogenic ability to invade host epithelial cells of many diverse bacterial genera ranging from the well-studied enterobacteria to *Neisseria* (23), *Porphyromonas* (21a), and beyond (27, 33). However, the depth of understanding of different bacterial invasion systems varies dramatically and is based primarily on studies of just a few specific pathogens (e.g., *Yersinia enterocolitica*, *S. typhimurium*, *Shigella flexneri*, and *Listeria monocytogenes* [11, 18, 24, 34]). Despite the tremendous worldwide public health significance of human typhoid fever, the limited understanding of *S. typhi* invasive ability was the impetus for these current physical studies.

Most cell culture studies of bacterial invasion have used starting bacterial MOIs of 10 to 100 (6, 14, 29). However, few studies have involved a kinetic analysis of an invasion system for the purpose of determining optimal MOIs, which might reveal unexpected features affecting bacterial invasion. Under our assay conditions, we discovered that bacterial concentrations were limiting for maximal *S. typhi* invasion efficiency at MOIs of <40 and became optimum at an MOI of ≃40. However, at MOIs of >40, where the bacterial numbers were not limiting, the invasion efficiency declined sharply. These data suggest a stringent limitation in host cell entry (e.g., limited entry sites or some other physical interference) at the higher MOIs tested here. Total numbers of *S. typhi* Ty2W bacteria internalized within 1 h leveled off at MOIs of ≥40, indicating that the host cell invasion machinery may be saturated at these bacterial numbers. For example, the addition of 4,000 Ty2W bacteria per host cell did not allow greater entry than an MOI of 40. Because all monolayer cells were shown by fluorescence microscopy to be infected after 60 min at MOIs of ≥40, we can state unambiguously that the number of internalized *S. typhi* bacteria averaged per epithelial cell reached a peak of 25 at an MOI of ≃400. The kinetics of invasion can vary significantly between different bacteria, under different assay conditions, and in different cell lines. For example, a previous study of enterohemorrhagic *E. coli* entry into T24 bladder epithelial cells showed a continual increase in internalized bacteria when the starting MOIs were increased from 2 to 2,000 and the number of internalized bacteria never reached a plateau (32). In contrast, Kusters et al. (21) found that maximal invasion by *S. typhimurium* occurred at an MOI of 100 after 60 min and resulted in two bacteria internalized per host cell. Such kinetic data allow a choice of optimal assay conditions to examine the invasion mechanism. The minimal *S. typhi* inocula needed to achieve maximal invasion efficiency (MOI of ≃40) and maximal number of internalized bacteria (MOI of ≃400) were used in further studies to analyze the Ty2W invasion process.

The relatively high invasion level observed for *S. typhi* Ty2W (~55% efficiency in a 1-h invasion assay) was obtained by growing the inoculum aerobically to mid-log phase in L broth containing 0.17 M NaCl, as reported by Tartera and Metcalf (40). This invasion level into INT407 cells was considerably higher than that reported by Mills and Finlay (28) for Ty2 grown under their optimal $O_2$-limiting conditions. The discrepancy in results, albeit important, may reflect strain differences, as Ty2W is a Vi capsule-negative Ty2 mutant which has previously been serially passaged through cell culture monolayers to select optimal invaders.

Previous studies have shown that *Salmonella* spp. bind to the apical surface of epithelial cells and trigger cytoskeletal rearrangements, resulting in bacterial uptake by a macropinocytic mechanism (1, 9, 14). Our kinetic studies have revealed a strict limitation on *S. typhi* entry. Is total apical surface area of INT407 cells limiting for bacterial interaction at MOIs of 40 to 4,000? The apical surface area of an average INT407 cell in monolayer under these conditions is 313 $\mu m^2$ ($1.88 \times 10^8$ $\mu m^2$ of area per well of 24-well plates divided by $6 \times 10^5$ INT407 cells per well). Using the reported average size of *S. typhi* (15), the approximate longitudinal area of the rod would be ~3.5 $\mu m^2$. We estimate that at least 50 flagellated bacterial cells placed longitudinally (or many more because bacteria bind at the tip of the rod) could potentially interact with the apical host cell surface at one time. Because SEM studies did not show monolayer cells accumulating large numbers of surface-bound bacteria, it is unlikely that the host cell apical surface area is limiting for bacterial interaction at MOIs of 40 to 4,000. Thus, the observed limitation on *S. typhi* Ty2W entry into INT407 cells at MOIs of >40 is not due simply to insufficient host cell surface area and may be due to a limited number of receptors or potential entry sites per host cell or perhaps some other effect on the host cell at higher MOIs.

Direct visualization studies quantitatively demonstrate the accuracy of the indirect, gentamicin kill viable count assay of bacterial invasion. Furthermore, these time course determinations of *S. typhi* invasion show that bacterial entry can be detected easily at 10 min postinfection. With time, the number of bacteria internalized increases until all monolayer cells are infected after 60 min at an MOI of 40. *S. typhi* entry was observed to occur more quickly over time at an MOI of ≃400, and all monolayer cells were infected within 30 to 35 min. Quite unexpectedly, direct visualization of the internalized bacteria over time revealed that they exist in two to three separate clusters per infected INT407 cell. At all time points postinfection at an MOI of ~400, the number of infection foci per cell still averaged 2 to 2.5 and the foci typically contained multiple bacteria per cluster. In addition, TEM studies indicated that one to two bacteria are typically engulfed per uptake event but that several consecutive uptake events may occur at the same activated membrane site (Fig. 4C). These data suggest that there are a limited number of potential *S. typhi* entry points (i.e., ~2 to 4) per INT407 cell, each of which results in an infection focus of one to several bacteria, depending on the

MOI. It is possible that there are infinite entry coordinates per cell but once specific factors are used up or activated at a few entry points, additional entry cannot take place elsewhere on that host cell.

EM studies allowed the examination of surface interactions and membrane structural alterations that occur over time during *S. typhi* internalization. As early as 10 to 20 min postinfection, one to three bacteria could be observed bound at the host cell surface to shortened microvilli in focal aggregates. Amplification of some focal aggregates showed one or several bacteria apparently bound to microvilli and tethered via other thinner appendages of undefined origin. Induced curly, hairlike structures observed previously (14) on *S. typhimurium* in contact with epithelial cells were not observed here. One striking feature of these *S. typhi*-infected monolayers was the occurrence of one to three focal aggregates of bound bacteria per cell regardless of the starting MOI, suggesting that a limited number of possible entry sites exist per cell. In contrast to the report of Yokoyama et al. (43), *S. typhi* did cause an alteration of host cell microvilli during bacterial entry as observed by EM. Infected host cells showed increased denuding (shortening and loss presumably due to F-actin depolymerization) of microvilli over time. Splash-like protrusions (or conical ruffles) of the INT407 apical membrane (observed by both SEM and TEM), likely due to F-actin rearrangement as previously reported (28), were triggered by some focal aggregates, and these events appeared to correlate with engulfment of centrally contained bacteria. The frequent finding of focal aggregates and macropinocytic structures adjacent to the tight junctions suggests that cognate receptors may be localized adjacent to the tight junction or migrating from the tight junction. Other small and large host cell membrane blebs or protrusions as well as surface bound bacteria could be seen in areas denuded of microvilli and were observed well after 1 h postinfection at an MOI of ≃400. Because our kinetic studies demonstrated that further *S. typhi* entry is essentially exhausted after this period, we speculate that these continuing membrane protrusions are not associated specifically with ongoing bacterial invasion but may be triggered by continued overstimulation of host cell signal transduction pathways and may result in the fluid filled macropinosomes seen at 60 to 120 min postinfection. Alternatively, the numerous vacuoles observed after 1 h postinfection may reflect events in host cell necrosis (29). These EM findings extend previous fluorescence microscopic observations (28) and limited EM analyses (4, 42, 43) of *S. typhi* invasion and show that the *S. typhi* entry process is very similar in appearance to the *S. typhimurium* invasion mechanism described previously (7, 8, 14, 37).

Kinetic analyses revealed a physical limitation on *S. typhi* internalization into INT407 cells which direct visualization and EM studies suggest could be the result of limited entry sites or receptors per cell. Alternatively, some other time-dependent change(s) (e.g., activated signaling pathways) in the host cell postinvasion may limit further bacterial uptake. Accordingly, prior invasion of a monolayer with Ty2W should deplete the host cells of entry sites and receptors over time. In fact, the $Km^r$ Ty2W was competitively inhibited by 2 to 3 logs in normal entry efficiency after monolayer preinfection with Ty2W. Although the host cell membrane shows major structural alterations by SEM after 30 to 45 min of preinfection with Ty2W, these alterations did not reduce host cell viability or inhibit the microfilament-dependent, *Yersinia* invasin-mediated entry pathway. In contrast, *S. typhimurium* was competitively inhibited by Ty2W, indicating that these two serovars may recognize the same major receptors in INT407 cells. This finding agrees with current evidence indicating that *Salmonella* serovars, including *S. typhi*, utilize a type III secretion system and an associated set of invasion proteins encoded in a 40-kb pathogenicity island to trigger invasion into the gut epithelium (11, 16). Despite these similarities, there are also preliminary indications of potential differences between *S. typhi* and *S. typhimurium* invasion processes. Elsinghorst et al. (4) described an *S. typhi* invasion gene region, now known to be physically separate from the well-studied Sip invasion system of several *Salmonella* serovars (16), and recent studies have shown that *S. typhi*, but not *S. typhimurium*, can utilize the cystic fibrosis transmembrane conductance regulator protein as a host invasion receptor (44). These observations open the possibility of multiple invasion pathways in *Salmonella* and multiple host invasion receptors.

*Shigella flexneri* and *Y. enterocolitica* share with *Salmonella* spp. many analogous genes involved in invasion and protein secretion (reviewed in reference 10). Since all of these genera trigger microfilament-dependent entry into host cells and members of the β1 integrin superfamily have been implicated as invasion receptors for both *Y. enterocolitica* (17) and *Shigella flexneri* (41), integrin involvement in *S. typhi* entry was examined. Monolayer pretreatments with various antibodies to β1 and certain specific heterodimers of β1 were found to inhibit *Yersinia* invasin-mediated entry but not *S. typhi* entry, providing limited evidence that integrins of the β1 superfamily are not involved as major *Salmonella typhi* invasion receptors in INT407 cells.

In conclusion, these kinetic and physical analyses of *S. typhi* invasion have revealed a strict and specific limitation on *S. typhi* entry into INT407 intestinal epithelial cells, which may be based on limited entry sites or receptors at the host cell membrane. Appreciation of this physical limitation will be vital to ongoing studies of the internalization process and the cognate epithelial receptors and *S. typhi* invasion ligands. A better understanding of the details of *S. typhi* invasion will augment our knowledge of its pathogenesis and hopefully will lead to new therapeutic and vaccine approaches.

## ACKNOWLEDGMENTS

We thank E. Elsinghorst and R. Isberg for kindly supplying bacterial strains, A. Jerse for advice on the AO-CV staining methodology, and K. Yamada for helpful advice and anti-integrin monoclonal antibodies.

X.-Z. Huang is a visiting research fellow of Fogarty International Center of the National Institutes of Health.

## REFERENCES

1. **Alpuche-Aranda, C. M., E. L. Racoosin, J. A. Swanson, and S. I. Miller.** 1994. *Salmonella* stimulate macrophage macropinocytosis and persist within spacious phagosomes. J. Exp. Med. **179:**601–608.
2. **Behlau, I., and S. I. Miller.** 1993. A PhoP-repressed gene promotes *Salmonella typhimurium* invasion of epithelial cells. J. Bacteriol. **175:**4475–4484.
3. **Clark, E. A., and J. S. Brugge.** 1995. Integrins and signal transduction pathway: the road taken. Science **268:**232–239.
4. **Elsinghorst, E., L. S. Baron, and D. J. Kopecko.** 1989. Penetration of human intestinal epithelial cells by *Salmonella*: molecular cloning and expression of *S. typhi* invasion determinants in *Escherichia coli*. Proc. Natl. Acad. Sci. USA **86:**5173–5177.
5. **Finlay, B. B.** 1994. Molecular and cellular mechanisms of *Salmonella* pathogenesis. Curr. Top. Microbiol. **192:**163–185.
6. **Finlay, B. B.** 1995. Interactions between *Salmonella typhimurium*, enteropathogenic *Escherichia coli* (EPEC), and host epithelial cells. Adv. Dent. Res. **9:**31–36.
7. **Finlay, B. B., and S. Falkow.** 1990. *Salmonella* interactions with polarized human intestinal Caco-2 epithelial cells. J. Infect. Dis. **162:**1096–1106.
8. **Finlay, B. B., B. Gumbiner, and S. Falkow.** 1988. Penetration of *Salmonella* through a polarized Madin-Darby canine kidney epithelial cell monolayer. J. Cell Biol. **107:**221–230.

8a. **Finlay, B. B., S. Chatfield, K. Y. Leung, G. Dougan, and S. Falkow.** 1991. Characterization of a *Salmonella choleraesuis* mutant that can not multiply within epithelial cells. Can. J. Microbiol. **37:**568–672.

9. **Francis, C. L., T. A. Ryan, B. D. Jones, S. J. Smith, and S. Falkow.** 1993.

Ruffles induced by *Salmonella* and other stimuli direct macropinocytosis of bacteria. Nature **364:**639–642.
10. **Galán, J. E.** 1994. Interaction of bacteria with non-phagocytic cells. Curr. Opin. Immunol. **6:**590–595.
11. **Galán, J. E.** 1996. Molecular genetic bases of *Salmonella* entry into host cells. Mol. Microbiol. **20:**263–271.
12. **Galán, J. E., and R. Curtiss III.** 1991. Distribution of the *invA*, *-B*, *-C*, and *-D* genes of *Salmonella typhimurium* among other *Salmonella* serovars: *invA* mutants of *Salmonella typhi* are deficient for entry into mammalian cells. Infect. Immun. **59:**2901–2908.
13. **Ginocchio, C., J. Pace, and J. E. Galán.** 1992. Identification and molecular characterization of a *Salmonella typhimurium* gene involved in triggering the internalization of *Salmonella* into cultured epithelial cells. Proc. Natl. Acad. Sci. USA **89:**5976–5980.
14. **Ginocchio, C. C., S. B. Olmsted, C. L. Wells, and J. E. Galán.** 1994. Contact with epithelial cells induces the formation of surface appendages on *S. typhimurium*. Cell **76:**717–724.
15. **Holt, J. G., N. R. Krieg, P. H. A. Sneath, J. T. Staley, and S. T. Williams.** 1994. Genus *Salmonella*, p. 175–289. *In* W. R. Hensyl (ed.), Bergey's manual of determinative bacteriology, 9th ed. The Williams & Wilkins Co., Baltimore, Md.
16. **Hueck, C. J., M. J. Hantman, V. Bajaj, C. Johnston, C. A. Lee, and S. Miller.** 1995. *Salmonella typhimurium* secreted invasion determinants are homologous to *Shigella* Ipa proteins. Mol. Microbiol. **18:**479–490.
17. **Isberg, R. R., and J. M. Leong.** 1990. Multiple β1 chain integrins are receptors for invasin, a protein that promotes bacterial penetration in mammalian cells. Cell **60:**861–871.
18. **Isberg, R. R., and G. T. V. Nhieu.** 1994. Two mammalian cell internalization strategies used by pathogenic bacteria. Annu. Rev. Genet. **27:**395–422.
19. **Kihlstrom, E.** 1977. Infection of HeLa cells with *Salmonella typhimurium* 395 MS and MR10 bacteria. Infect. Immun. **17:**290–295.
20. **Kohbata, S., H. Yokoyama, and E. Yabuuchi.** 1986. Cytopathogenic effect of *Salmonella typhi* GIFU 10007 on M cells of murine ileal Peyer's patches in ligated ileal loops: an ultrastructural study. Microbiol. Immunol. **30:**1225–1237.
21. **Kusters, J. G., G. A. W. M. Mulders-Kremers, C. E. M. van Doornik, and B. A. M. van der Zeijst.** 1993. Effects of multiplicity of infection, bacterial protein synthesis, and growth phase on adhesion to and invasion of human cell lines *by Salmonella typhimurium*. Infect. Immun. **61:**5013–5020.
21a. **Lamont, R. J., A. Chan, C. M. Belton, K. T. Izutsu, D. Vasel, and A. Weinberg.** 1995. *Porphyromonas gingivalis* invasion of gingival epithelial cells. Infect. Immun. **63:**3878–3885.
22. **Lee, C. A., B. D. Jones, and S. Falkow.** 1992. Identification of a *Salmonella typhimurium* invasion locus by selection for hyperinvasive mutant. Proc. Natl. Acad. Sci. USA **89:**1847–1851.
23. **Makino, S., J. P. van Putten, and T. F. Meyer.** 1991. Phase variation of the opacity outer membrane protein controls invasion by *Neisseria gonorrhoeae* into human epithelial cells. EMBO J. **10:**1307–1315.
24. **Mengaud, J., H. Ohayon, P. Gounon, R.-M. Mege, and P. Cossart.** 1996. E-cadherin is the receptor for internalin, a surface protein required for entry of *L. monocytogenes* into epithelial cells. Cell **84:**923–932.
25. **Miliotis, M. D.** 1991. Acridine orange stain for determining intracellular enteropathogens in HeLa cell. J. Clin. Microbiol. **29:**830–831.
26. **Miliotis, M. D., H. J. Koornhof, and J. I. Phillips.** 1989. Invasive potential of noncytotoxic enteropathogenic *Escherichia coli* in an in vitro Henle 407 cell model. Infect. Immun. **57:**1928–1935.
27. **Miliotis, M. D., B. D. Tall, and R. T. Gray.** 1995. Adherence to and invasion of tissue culture cells by *Vibrio hollisae*. Infect. Immun. **63:**4959–4963.
28. **Mills, S. D., and B. B. Finlay.** 1994. Comparison of *Salmonella typhi* and *Salmonella typhimurium* invasion, intracellular growth and localization in cultured human epithelial cells. Microb. Pathog. **17:**409–423.
29. **Monack, D. M., B. Raupach, A. E. Hromockyj, and S. Falkow.** 1996. *Salmonella typhimurium* invasion induces apoptosis in infected macrophages. Proc. Natl. Acad. Sci. USA **93:**9833–9838.
30. **Mroczenski-Wildey, M. J., J. L. Di Fabio, and F. C. Cabello.** 1989. Invasion analysis of Hela cell monolayers by *Salmonella typhi*: the role of lipopolysaccharide. Microb. Pathog. **6:**143–152.
31. **Oelschlaeger, T. A., and B. D. Tall.** 1996. Uptake pathways of clinical isolates of *Proteus mirabilis* into human epithelial cells. Microb. Pathog. **20:**1–16.
32. **Oelschlaeger, T. A., T. J. Barrett, and D. J. Kopecko.** 1994. Some structures and processes of human epithelial cells involved in uptake of enterohemorrhagic *Escherichia coli* O157:H7 strains. Infect. Immun. **62:**5142–5150.
33. **Oelschlaeger, T. A., P. Guerry, and D. J. Kopecko.** 1993. Unusual microtubule-dependent endocytosis mechanisms triggered by *Campylobacter jejuni* and *Citrobacter freundii*. Proc. Natl. Acad. Sci. USA **90:**6684–6688.
34. **Ogawa, H., A. Nakamura, and R. Nakaya.** 1968. Cinemicrographic study of tissue cell cultures infected with *Shigella flexneri*. Jpn. J. Med. Sci. Biol. **21:**259–273.
35. **Pang, T., Z. A. Bhutta, B. B. Finlay, and M. Altwegg.** 1995. Typhoid fever and other salmonelloses: a continuing challenge. Trends Microbiol. **3:**253–255.
36. **Pegues, D. A., M. J. Hantman, I. Behlau, and S. I. Miller.** 1995. PhoP/PhoQ transcriptional repression of *Salmonella typhimurium* invasion genes: evidence for a role in protein secretion. Mol. Microbiol. **17:**169–181.
37. **Portillo, F. G., and B. B. Finlay.** 1994. *Salmonella* invasion of nonphagocytic cells induces formation of macropinosomes in the host cell. Infect. Immun. **62:**4641–4645.
38. **Takeuchi, A.** 1967. Electron microscope studies of experimental *Salmonella* infection. Penetration into the intestinal epithelium by *Salmonella typhimurium*. Am. J. Pathol. **50:**109–136.
39. **Tall, B. D., R. T. Gray, and D. B. Shah.** 1993. Bacterial adherence and biofilm behavior of *Vibrio vulnificus*, p. 378–379. *In* G. W. Bailey and C. L. Rieder (ed.), Proceedings of the Annual Meeting of the Microscopy Society of America. San Francisco Press, Inc., San Francisco, Calif.
40. **Tartera, C., and E. Metcalf.** 1993. Osmolarity and growth phase overlap in regulation of *Salmonella typhi* adherence to and invasion of human intestinal cells. Infect. Immun. **61:**3084–3089.
41. **Watarai, M., S. Funato, and C. Sasakawa.** 1996. Interaction of Ipa proteins of *Shigella flexneri* with α5β1 integrin promotes entry of the bacteria into mammalian cells. J. Exp. Med. **183:**991–999.
42. **Yabuuchi, E., M. Ikedo, and T. Ezaki.** 1986. Invasiveness of *Salmonella typhi* strains in Hela S3 monolayer cells. Microbiol. Immunol. **30:**1213–1224.
43. **Yokoyama, H., M. Ikedo, and S. Kohbata.** 1987. An ultrastructural study of Hela cell invasion with *Salmonella typhi* GIFU 10007. Microbiol. Immunol. **31:**1–11.
44. **Zaidi, T. S., M. Grout, C. Lee, and G. B. Pier.** 1997. *Salmonella typhi*, but not *S. typhimurium*, enters epithelial cells via the cystic fibrosis transmembrane conductance regulator (CFTR), abstr. D-98, p. 225. *In* Abstracts of the 97th General Meeting of the American Society for Microbiology 1997. American Society for Microbiology, Washington, D.C.

*Editor:* V. A. Fischetti